JCSE The Journal of Corrosion Science and Engineering
ISSN 1466-8858 Volume 12, Preprint 42 submitted 30 June 2010

The Effect of Sulphate on the Electrochemical Behaviour of a Cu-Ni-Fe alloy (C70600)

A. Taher, G. Jarjoura and G. J. Kipouros

Materials Engineering Programme
Dalhousie University
1360 Barrington Street, Halifax, Nova Scotia
B3J 2X4

Email: georges.kipouros@dal.ca

Abstract

The electrochemical behaviour of a 90% Cu-10% Ni-1.1% Fe (C70600) commercial alloy in natural sea water and in artificial saline solutions with different sulphate concentrations was investigated. The measurements were conducted in aerated electrolytes at room temperature. Cyclic voltammetry (CV), Tafel extrapolation (TE), cyclic polarization (CP), and linear sweep polarization (LSP) techniques were preformed in this investigation. The corrosion products and the passive film were analyzed using a field emission scanning electron microscope (FE-SEM), electron probe microanalysis (EPMA), energy dispersive spectrometry (EDS), wavelength dispersive spectrometry (WDS), and X-Ray diffraction (XRD). The corrosion behaviour depends on the amount of sulphate in the artificial saline solution. Sulphate amounts above 400 ppm in the artificial saline electrolyte limit the ability of the passive film to protect the alloy. The behaviour of the alloy in the sea water environment is very similar to the behaviour of the alloy in the 2260 ppm sulphate artificial saline solution. In solution that contained no sulphate the passive film consists mainly of chlorides. The presence of sulphate in corrosive solutions produces a passive layer containing mainly chlorides and sulphides (FeS, NiS, and CuS).

Key words: corrosion, copper-nickel alloys, sulphate, sea water.

JCSE The Journal of Corrosion Science and Engineering
ISSN 1466-8858 Volume 12, Preprint 42 submitted 30 June 2010

Introduction

Due to excellent resistance to corrosion and biofouling, the copper-nickel alloys are used extensively in marine applications. The corrosion resistance is improved by increasing the nickel content in Cu-Ni alloys, but the biofouling resistance in the marine environment decreases. The most common alloys used in marine environments which exhibit both excellent corrosion and biofouling resistance are the
90 w% Cu-10 w% Ni and 70 w% Cu-30 w% Ni alloys [1].

The protective film can be formed in marine environment only if there is a stagnant environmental condition or the corrosive fluid is in a slow movement**,** and the most common corrosion products in the marine environment are cupric oxychloride, cupric hydroxide, basic cupric carbonate, and cuprous oxide [1]. Powell [2] concluded that exposure of 90% Cu-10% Ni alloys initially in clean sea water for a period between few hours and few months, depending on the temperature and the type of the alloy, is important to form a good protective film on the surface. These surface films consist of multi layers of cuprous oxide, and may contain other compounds such as nickel oxide, iron oxide, cuprous hydroxide and cupric oxide. The films may be of different colour such as brown, greenish brown or brownish black depending on the thickness and the chemical compounds present in the film. B. Syrett [3] studied the electrochemical behaviour of copper- nickel alloys in a marine environment. The protective thin layer of Cu_2O which is formed on the surface is doped with some other alloying elements that were originally available as alloy additions such as Ni, Fe and possibly Mn. In polluted environments the layer is also doped with other elements from the solution such as S, Si

ISSN 1466-8858. Volume 12, Preprint 42 submitted 30 June 2010

and sometimes Cl, Mg and Ca. In addition to Cu_2O, $Cu_2(OH)_3Cl$ may also be present. The corrosion rate is not accelerated for the Cu-Ni alloys in deaerated sea water, but there is an increase in the corrosion rate after the polluted environment has been replaced by aerated unpolluted seawater. It was proposed by B. Syrett [3] that the reason of the increased corrosion rate was the change of the cathodic reaction from H^+ ion reduction to oxygen reduction which led to an increase of the cathodic reaction rate and thus the overall corrosion rate increased.

Efird [4] has produced a Pourbaix diagram for the 90 w% Cu-10 w% Ni alloy in sea water and provided data on immunity, passivation, corrosion, and dealloying susceptibility regions. According to this study, the passivation process takes place for a 90 w% Cu-10 w% Ni alloy in sea water at pH values higher than 8.5. At pH values less than 8.5, the corrosion product precipitates from the solution on the surface of the alloy. By increasing the exposure time, the value of pH which causes the precipitation / passivation transformation mechanism decreased because the surface of the 90 w% Cu-10 w% Ni alloy becomes enriched with nickel.

P. Druska et al [5] studied the nature of the passive layer which formed on a 90 w% Cu-10 w% Ni alloy in alkaline solutions in the absence of sulphur. The passive film layer depended on the exposure time and the potential value and did not have a simple structure. $Ni(OH)_2$ was formed in the early step immediately after immersing the alloy in alkaline solutions (at negative potential values) followed by the formation of Cu_2O leaving the surface enriched with nickel which oxidizes to NiO and takes a location as an inner layer. At high potential (after sufficient time), the Cu_2O layer oxidizes to CuO

ISSN 1466-8858 Volume 12, Preprint 42 submitted 30 June 2010

/$Cu(OH)_2$. This oxidation process takes place at the transpassive region. Also $Ni(OH)_2$ will oxidize to NiOOH and will take a position in the outer layer with $Cu(OH)_2$.

S. Sayed et al [6] reported that the corrosion rate of 90 w% Cu-10 w% Ni alloys in a de-aerated solution varied between 1.8 mpy (0.046 mmpy) in the absence of sulphide ions in a NaCl solution and 7.73 mpy (0.196 mmpy) in solutions that contained 1000 ppm sulphide. The protective layer in the absence of sulphide ions was black in colour covered with a porous green layer. In the presence of sulphide ions, the colour of the original alloy lost its brightness. Addition of sulphide ions generally increased the corrosion and the pitting corrosion. Copper sulphide, Cu_2S, was formed along with the protective film (Cu_2O) and $Cu_2(OH)_3Cl$. The formation of Cu_2S increased the corrosion rate because it permitted rapid ionic and electronic transport through the protective layer. The corrosion rate of the C70600 alloy (88.85 w% Cu, 10.21 w% Ni, 0.58 w% Mn, 0.31 w% Mg, 0.05 w% Al) in artificial sea water without sulphate content (3.75 w% NaCl, 0.45 w% $CaCl_2$, $MgCl_2$) was 0.05 mmpy [7]. Based on the electrochemical impedance spectroscopy (EIS) results, the corrosion rate decreased with increasing the immersion time under stagnant conditions [7]. In unpolluted sea water [8], the corrosion rate of the 90 w% Cu-10 w% Ni alloy is affected by variables such as the oxygen content of the water and the velocity of the water flow. In aerated quiescent conditions, the corrosion rate of the 90 w% Cu-10 w% Ni alloy is 0.695 mpy (0.018 mmpy) and increased to 1.33 mpy (0.034 mmpy) in deaerated condition. In a stirred condition, the corrosion rate was recorded to be 2.67 mpy (0.068 mmpy) and 26.9 mpy (0.759 mmpy) for aerated and deaerated conditions, respectively. The decrease in the corrosion rate in the aerated environment was attributed by the authors to the formation of a protective film.

JCSE The Journal of Corrosion Science and Engineering
ISSN 1466-8858 Volume 12, Preprint 42 submitted 30 June 2010

Sulphur can be found in the corroding environment as sulphuric or sulphurous acid. Both increase the corrosion rate, but sulphuric acid causes more severe increase in the corrosion rate. It was reported that the corrosion rate of copper-nickel alloys reached 0.3 ipy (7.62 mmpy) in aerated sulphuric acid solution with concentration of 10 w%, but in the absence of oxygen it was only 0.03 ipy (0.762 mmpy) [9]. A piece of the C70600 alloy was attached on a ship body, and the corrosion rate was recorded to be approximately 0.025 mmpy in the natural sea water after long exposure time (14 months). When the piece was insulated from the ship body (to avoid the galvanic effect), the corrosion rate was about 0.08 mmpy [10].

Dhar et al [11] investigated the behaviour of the 90 w% Cu-10 w% Ni alloys in both 0.5 M NaCl solution with pH of 6.5, and synthetic sea water (SSW) with pH of 8.2. Even though the current density and the corrosion rate recorded to be lower in case of using the SSW, the corrosion behaviour in both environments was based on the reaction

$$Cu + 2Cl^- \rightarrow CuCl_2^- + e^- \quad (1)$$

K. Ismail et al [12] studied the electrochemical behaviour of copper - nickel alloys including the commercial 90 w% Cu-10 w% Ni alloy by different electrochemical techniques in alkaline sulphate solution (0.25 M $NaSO_4$ + 0.01 M NaOH, pH =12). They found that by increasing the sulphate ion concentration in the solutions up to 0.25M will cause a decrease in the passivity, but if the sulphate concentration increased more

ISSN 1466-8858 Volume 12, Preprint 42 submitted 30 June 2010

than this value, the passivity was improved. CuO and Cu_2O peaks were present in all the corrosion films of copper nickel alloys.

El-Domiaty et al [13] investigated the effect of sulphide ions on the stress corrosion cracking (SCC) of the 90 w% Cu- 10 w% Ni alloy; it was found that the susceptibility to SCC increased as the sulphide concentration increased. The general corrosion of copper-nickel alloy was also increased with increasing the sulphide content due to selective copper dissolution.

The behaviour of 90 w% Cu-10 w% Ni alloys in neutral sulphate solutions was studied by Ismail et al. [14] and it was concluded, based on the EIS results, that the passive film resistance increased with the immersion time of alloys in these solutions. In the polluted sea water systems with pH ranging between 5.5 and 7.5 [15], Cu_2S is incorporated in the Cu_2O and results in a less protective film compared to that formed in unpolluted sea water. The film starts to behave as a cathode with respect to the base material, and the corrosion process takes the form of pitting corrosion. Even a small amount of sulphide (0.05 ppm) is sufficient to increase the corrosion rate of 90 w% Cu-10 w% Ni alloys.

In the clean water of Atlantic Ocean [16], the corrosion potential was determined to be -285 mV/SCE for a 90 w% Cu-10 w% Ni alloy and the pitting potential was -40 mV/SCE, but by increasing the sulphide content to 1 ppm, the corrosion and the pitting potential were -230 mV/SCE and -50 mV/SCE, respectively. This means that the passivity range decreased by increasing the sulphide in the sea water and the pitting potential comes closer to the corrosion potential.

ISSN 1466-8858 Volume 12, Preprint 42 submitted 30 June 2010

No comprehensive study in a wide range of sulphate content has been reported. The sulphate content varies in different marine environments. The objective of this study was to investigate the effect of sulphate concentration on the electrochemical behaviour of the Cu-10% Ni-1.1% Fe (C70600) alloy. North Atlantic Ocean environment and artificial saline solutions containing 2.86 w% NaCl and 0, 50, 100, 200, 300, 400, 500, 600, 700, 800, 1000, and 2260 ppm sulphate were used.

Experimental Procedure

Materials

Commercial alloy C70600 samples were cut using a hole saw from a 1/8″ thick plate. The surface of the samples was ground using 240, 320, 400 and 600 grit SiC papers and polished using 1 and 0.05 micron alumina suspensions followed by cleaning ultrasonically in a distilled water bath. The commercial alloy was analyzed by Atomic Absorption (AA) and Inductively Coupled Plasma (ICP), and its chemical composition is shown in Table 1.

Table 1. The chemical composition of commercial Cu-Ni-Fe alloy C70600.

Element	Cu	Ni	Fe	Zn	Na	Al	Cr	Mn	K	Mo	Co
Wt %	88.62	9.86	1.11	0.13	0.22	0.006	0.001	0.001	0.017	0.01	0.005

Electrolytes

Nova Scotia (N.S.) sea water was used as an electrolyte. It was analyzed because there were no comprehensive data about the chemical analysis of the sea water in this

ISSN 1466-8858 Volume 12, Preprint 42 submitted 30 June 2010

part of the Atlantic Ocean. Table 2 shows the chemical analysis of a water specimen which was taken from a small village called Peggy's Cove to avoid sources of contamination. This composition was confirmed several times in the duration of this experimental work.

Table 2. The chemical composition Nova Scotia sea water.

Element/Substance	Cl	Na	SO_4^{2-}	K	Mg	Ca	F	Fe	Rb
Amount (ppm)	17400	8460	2260	316	105	33	29	0.34	0.22

Artificial saline solutions were prepared using distilled water to which were added 2.86 wt% NaCl and 0, 50, 100, 200, 300, 400, 500, 600, 700, 800, 1000, and 2260 ppm sulphate. All experiments were carried out in aerated electrolytes and at room temperature (22 ^{o}C ±1.1 ^{o}C). A traceable digital Oxygen Meter provided by Fisher Scientific was used to evaluate the dissolved oxygen in sea water and the artificial solutions; the average oxygen dissolved was 8.2 mg/L. The pH of the natural sea water was 7.8, and for the synthetic saline solution ranged between 4.76 and 6.75 depending on the sulphate content.

Electrochemical Measurements

A potentiostat model 273A (EG & G, Princeton Applied Research) was used for different electrochemical techniques including Tafel extrapolation, linear sweep polarization, cyclic voltammetry, and cyclic polarization. The potentiostat was controlled by Corrware software. A three-electrode electrochemical cell was used (the standard

ISSN 1466-8858 Volume 12, Preprint 42 submitted 30 June 2010

commercial type) for all the electrochemical measurements. Only 1 cm^2 of the sample surface was subjected to the electrolyte through a hole by mounting the sample in a Teflon holder. That facilitated the conversion of the measured current to current density. A graphite rod with a surface area of 16.32 cm^2 was used as counter electrode and a saturated calomel electrode (SCE) was used as a reference electrode.

Table 3 shows the potential the range versus SCE and the scanning rate for all the electrochemical techniques which were used in this work.

Table 3. Electrochemical techniques, potential range versus SCE and scanning rate

Electrochemical technique	Potential range versus SCE	Scanning rate
Linear sweep polarization (LSP)	-0.25 to 0.75 V	1 mV/S
Cyclic polarization (CP)	-1.5 to 2.5 V	1 mV/s
Tafel Extrapolation (TE)	-0.5 V to 0.02 V	1 mV/s
Cyclic voltammetry (CV)	-1.50 to 1.50 V	10 mV/s

Surface Characterization

A Hitachi S-4700 Field Emission Scanning Electron Microscope (FE-SEM) equipped with EDS, a Joel JXA-8200 Electron Probe Micro Analyzer (EPMA) attached to both energy dispersive spectrometer (EDS) and wavelength dispersive spectrometer (WDS), and a D8 Advance X-ray generator and diffractometer (Bruker axs, Model Advance D8) were used to analyze the corrosion product and the passive films qualitatively and quantitatively.

JCSE The Journal of Corrosion Science and Engineering
ISSN 1466-8858 Volume 12, Preprint 42 submitted 30 June 2010

Results and Discussion

Tafel Extrapolation and corrosion rates

The corrosion film produced in all electrolytes was consisting of two layers, the inner layer, which is golden-brown in colour, porous, and has a good adhesion to the substrate surface, and the outer, which is a black colour layer, cracked, and has poor adhesion. Similar surface features were observed by previous authors [2, 6]. Based on the XRD, EDS and WDS results in this study, the passive film detected was consisting of $Cu_2(OH)_3Cl$, CuCl, and $Ni(ClO_4)_2.6H_2O$ when artificial saline solution was used without sulphate content. When sulphate was added to the solution or in N.S. sea water, FeOCl, CuS, FeS, and NiS were detected in addition to the three compounds which detected when using a solution without sulphate. XRD spectra of C70600 commercial alloy in NaCl artificial solutions with and without sulphate and in sea water are shown in Figure 1.

The corrosion rate was calculated for samples in different electrolytes using Tafel Extrapolation. The cathodic slope and the anodic slope constants, the corrosion potential, and the corrosion current were estimated from the Tafel plots as seen in Figure 2. The corrosion rate was initially decreased by increasing the amount of sulphate in the solution from 0 ppm to 400 ppm, and then increased drastically. The corrosion rate ranged from 0.03 mmpy in the 0 ppm sulphate artificial saline solution to 0.046 mmpy in the sea water environment as can be seen in Table 4. Similar results are obtained for the same alloy in a previous study (0.03 mmpy) at very low concentration of sulphide (0.01 mg/L) [17]. It was reported that the corrosion rate in the absence of sulphate was 0.048 mmpy [18], 0.043 mmpy [6], 0.03 mmpy [7], and 0.023 mmpy [8]. G. Kear et al [19] reported that

the corrosion rate varied between 0.01 mmpy and 0.24 mmpy. When adding sulphate up to 600 ppm, there was no significant change in the corrosion rate values, but if more than 600 ppm were added to the solution, the corrosion rate increased to a relatively high value. Addition of sulphate to 1000 ppm caused the corrosion rate to be 0.039 mmpy. The corrosion rate calculations were 0.042 and 0.046 mmpy for both 2260 ppm sulphate and the N. S. sea water, respectively.

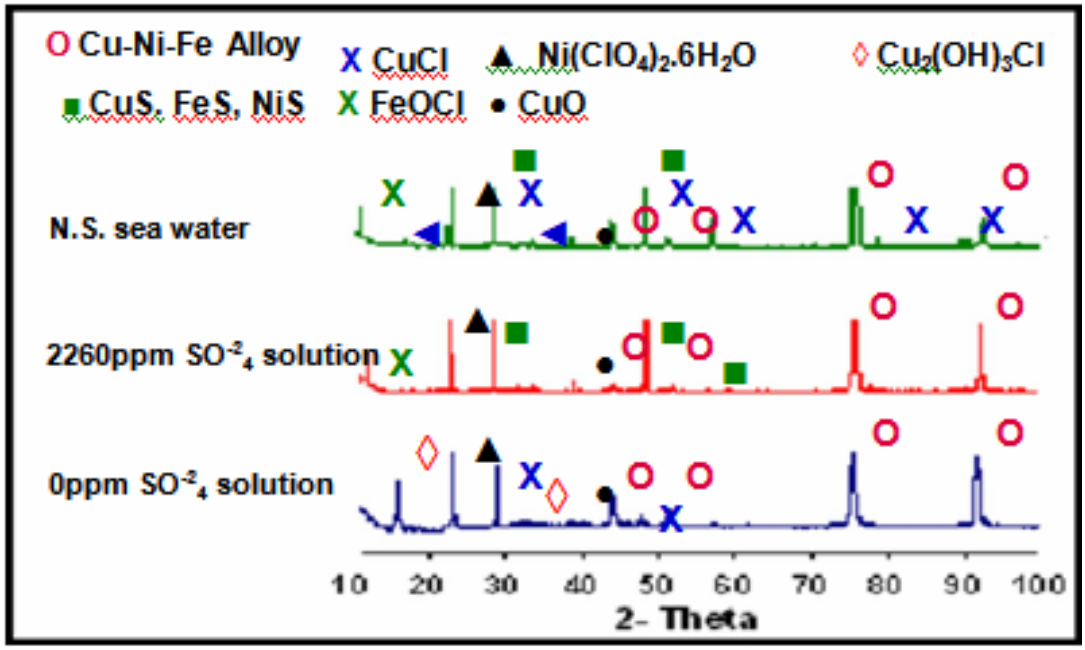

Figure 1. XRD spectra of C70600 exposed to different environments.

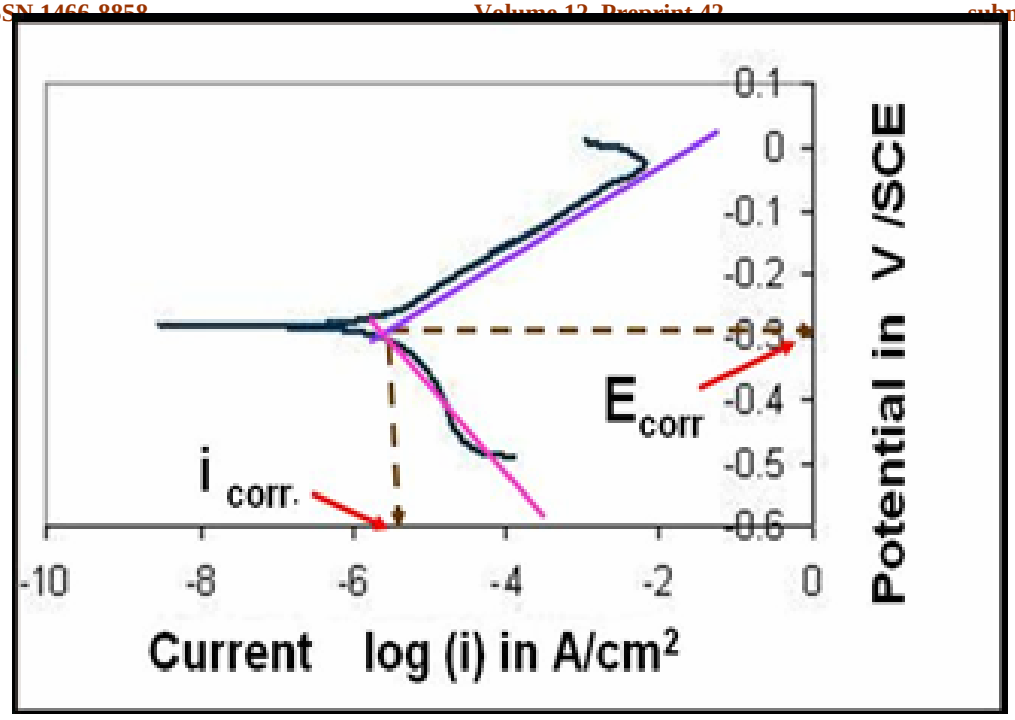

Figure 2. Tafel extrapolation of commercial C70600 in 0 ppm sulphate artificial saline solution.

Table 4. The corrosion rate of commercial alloy C70600 in various artificial saline solutions and in N.S. sea water.

Solution	*Corrosion rate (mmpy)*	*Solution*	*Corrosion rate (mmpy)*
0 ppm sulphate	0.030	600 ppm sulphate	0.027
100 ppm sulphate	0.029	700 ppm sulphate	0.035
200 ppm sulphate	0.030	800 ppm sulphate	0.040
300 ppm sulphate	0.026	1000 ppm sulphate	0.039
400 ppm sulphate	0.025	2260 ppm sulphate	0.042
500 ppm sulphate	0.027	N.S. sea water	0.046

ISSN 1466-8858 Volume 12, Preprint 42 submitted 30 June 2010

The linear polarization plots for the commercial alloy C70600 in different artificial saline solutions and in N.S. sea water are shown in Figure 3. The electrochemical behaviour of the commercial alloy depends on the amount of sulphate in the solution. In the absence of sulphate in the artificial saline solution, plot a, and at low concentrations of sulphate (less than 400 ppm), the C70600 alloy has a good passivity in the range of potential values from +0.1 V/SCE to +0.75 V/SCE. This can be explained by the decrease in the passivation current density value at +0.1 V/SCE to a lower value which remains approximately constant until the potential reaches the value of +0.75 V/SCE. This indicates that the passive film has good integrity and there is very limited or no pitting corrosion at low sulphate concentrations to destroy the passivity of the film. The current density value increased with the addition of sulphate up to 400 ppm. Similar results in 0 ppm sulphate artificial saline solution were also reported in another study [20].

By increasing the sulphate content of the solution to more than 400 ppm, a transpassive region appeared starting from the potential of +0.65 V/SCE for the 400 ppm sulphate artificial saline solution. This transpassive region is evidence of the breakdown of the passive film and the current density starts to increase again. The value of the transpassive potential was observed to decrease with increasing amount of sulphate above the 400 ppm value up to the maximum sulphate concentration solution of 2260 ppm. The transpassive potential value was +0.50 V/SCE for the commercial alloy in the 800 ppm sulphate artificial saline solution, and it was approximately +0.47 V/SCE in the 2260

ppm sulphate artificial saline solution and the N.S. sea water. This results in a decrease in the passivity potential range (the difference between the passivation potential and the transpassive potential value). In addition to the change in the potential values, the passivation current density values were increased by raising the amount of sulphate above 400 ppm. This indicates that the alloy is more active and the passive layer becomes less protecting at high sulphate concentrations. The behaviour of the commercial alloy in the N.S. sea water environment was very close to the behaviour of the alloy in the 2260 ppm sulphate artificial saline solution.

Cyclic polarization and the protection potential

Figure 4 shows the cyclic polarization plots for commercial alloy C70600 in artificial saline solutions containing various amounts of sulphate and in N.S. sea water. The electrochemical behaviour of the commercial alloy depends on the amount of sulphate in the solution. By adding sulphate to the solution up to 400 ppm, the potential difference between the corrosion potential (varied between -0.401 V/SCE and -0.409 V/SCE) and the protection potential (varied between -0.138 V/SCE and -0.144 V/SCE) remains approximately the same. By adding more than 400 ppm of sulphate, the potential difference becomes smaller (for example, the difference becomes 0.231 V/SCE in 2260 ppm sulphate artificial saline solution compared to 0.263 V/SCE when 0 ppm sulphate artificial saline solution was used), which indicates that the commercial alloy becomes less protected. This result is consistent with the results obtained by the linear polarization technique where 400 ppm of sulphate led to a significant change in the behaviour of the alloy.

ISSN 1466-8858 Volume 12, Preprint 42 submitted 30 June 2010

The smallest potential difference was observed for the commercial alloy in the 2260 ppm artificial saline solution and in the N.S. sea water. The protection potential values remained approximately the same for the alloy in all of the environments; it varied between -0.138 V/SCE and -0.145 V/SCE. On the other hand, the corrosion potential shifted to more negative values in the solution containing up to 400 ppm sulphate (from -0.401 V/SCE in the 0 ppm sulphate artificial saline solution to -0.409 V/SCE in the 400 ppm sulphate artificial saline solution). Starting in artificial saline solution with 400 ppm sulphate as an electrolyte, the corrosion potential starts shifting to less negative values. It was about -0.391 V/SCE in the 600ppm sulphate artificial saline solution, -0.373 V/SCE in the 2260 ppm sulphate artificial saline solution and approximately -0.375 V/SCE in the N.S. sea water. In contrast to results obtained by another study [21], the corrosion potential for the commercial alloy in N.S. sea water was -0.220 V/SCE but the electrolyte (the sea water) was not in stagnant condition as it is in the current study, the flow velocity of the sea water was 0.5 m/s. The behaviour of the commercial alloy in the 2260 ppm artificial saline solution was the same with that of the commercial alloy in the N.S. sea water, and these plots were similar to those reported by others [13].

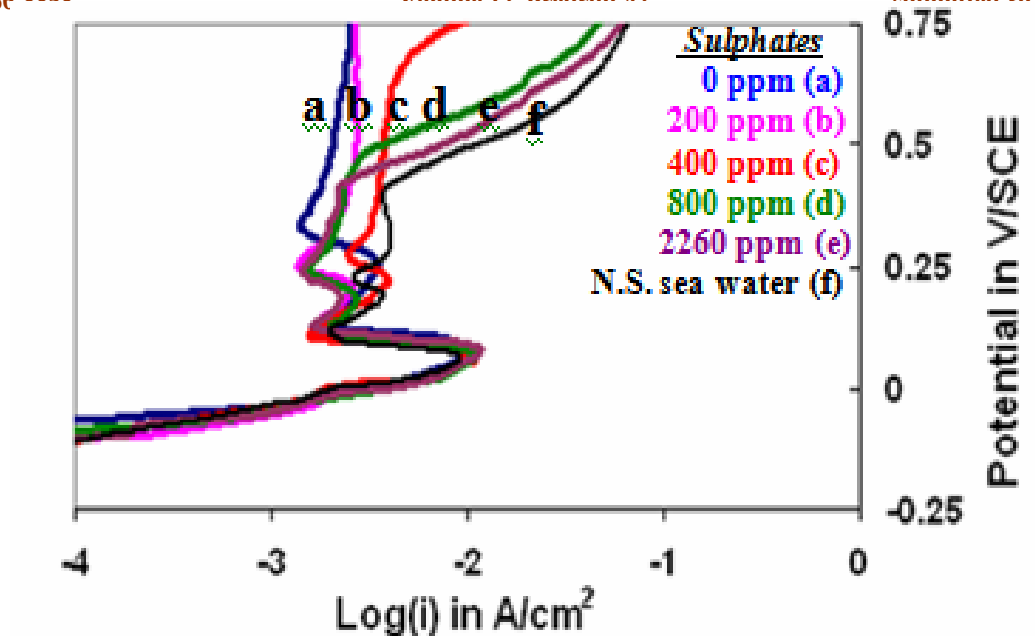

Figure 3. Linear sweep polarization plots for commercial alloy C70600 in N.S. sea water and in artificial saline solutions and for various concentrations of sulphates

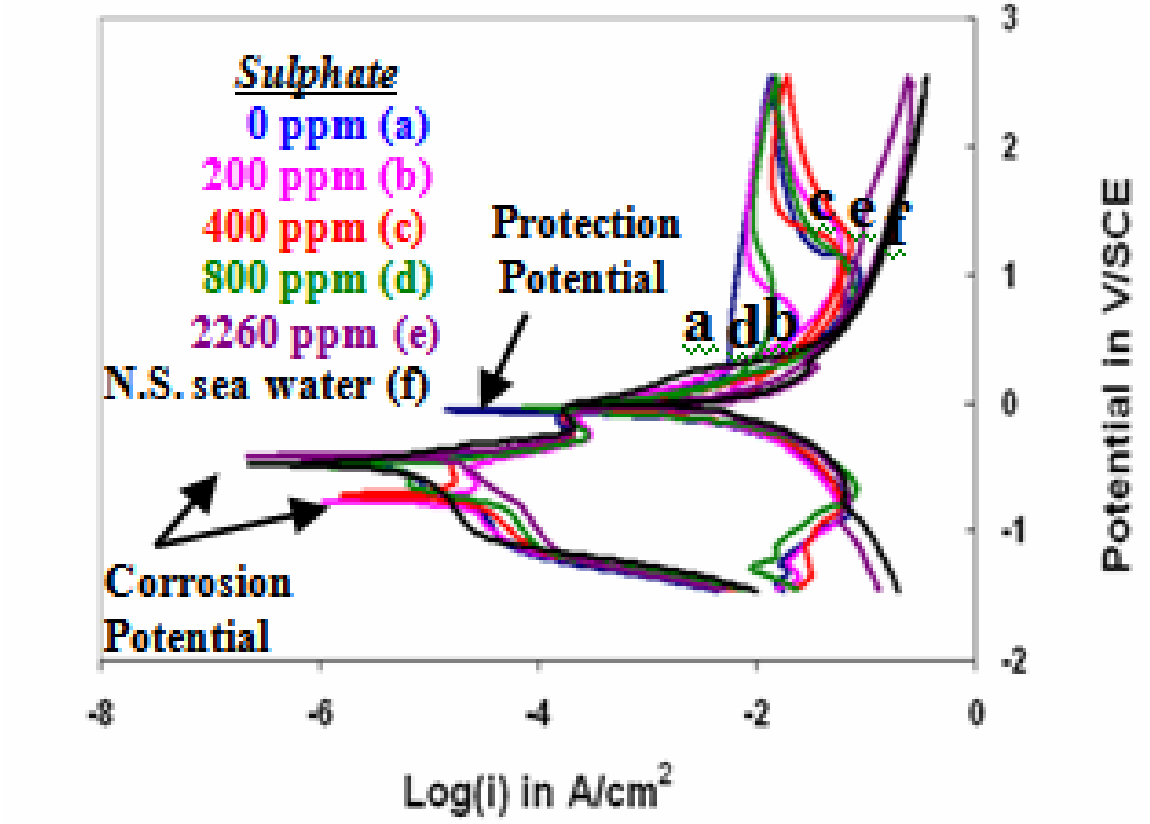

Figure 4. Cyclic Polarization plots for commercial alloy C70600 in artificial saline solutions for various concentrations of sulphates and N.S. sea water

ISSN 1466-8858 Volume 12, Preprint 42 submitted 30 June 2010

Cyclic voltammetry

Cyclic voltammetry was used to determine the mechanism of the corrosion process of the commercial alloy C70600 in the solutions under consideration. Figure 5 shows the voltammograms of the commercial alloy in 0 ppm sulphate artificial saline solution and 200 ppm sulphate artificial saline solution. The 0 ppm voltammogram is similar to one produced in a previous study for a 85 w% Cu-15 w% Ni alloy [22]. The results clearly show that the reactions taking place in this system are not ideally reversible because the anodic current peaks are not equal to the cathodic current peaks, the separation between the anodic and the cathodic potentials (E_{pa} - E_{pc}) at room temperature is not equal to 59/n mV. It can be seen that there are more than one anodic peaks in the area of the anodic polarization and also there were more than one peaks in the region of cathodic polarization in the 0 ppm sulphate artificial saline solution environment. There were two anodic peaks (A1 and A2) which had potential values of +0.331 V/SCE and +0.58 V/SCE. There were four cathodic peaks (C1, C2, C3, and C4) which had the following potential values +0.137 V/SCE, +0.061 V/SCE, -0.438 V/SCE, and -0.522V/SCE, respectively. This indicates that there was more than one reaction taking place on the surface of the alloy in this environment. The peaks that appear in the anodic region could be attributed to the following reactions:

$$2Cu + H_2O \rightarrow Cu_2O + 2H^+ + e^- \quad (2)$$

$$Cu_2O + ½\ O_2 + Cl^- + 2H_2O \rightarrow Cu_2(OH)_3Cl + OH^- \quad (3)$$

ISSN 1466-8858 Volume 12, Preprint 42 submitted 30 June 2010

One of the cathodic peaks which has the potential value of -0.438 V/SCE could be attributed to the reduction of $Cu_2(OH)_3Cl$ by the reaction:

$$Cu_2(OH)_3Cl + OH^- \rightarrow Cu_2O + \tfrac{1}{2} O_2 + Cl^- + 2H_2O \quad (4)$$

Adding sulphate to the artificial saline solution (200 ppm), more peaks appeared in the voltammogram, which indicates that more reactions took place (involving sulphur) during the corrosion process. There were four anodic peaks in the voltammogram of the alloy instead of two observed in 0 ppm sulphate artificial saline solution. The four anodic peaks had +0.317 V/SCE, +0.507 V/SCE, +0.643 V/SCE, and +0.817 V/SCE potential values, respectively. In the 200 ppm sulphate artificial saline solution, four cathodic peaks also occurred. The potential values of theses four peaks are +0.086 V/SCE, +0.06 V/SCE, -0.44 V/SCE, and -0.774 V/SCE, respectively.

It can be observed that adding 200 ppm of sulphate to the solution caused a small shift in the potential positions of peaks A1 and A2 to lower values compared to the same peaks in the 0 ppm solution. The potential positions of the three cathodic peaks (C1, C2, and C3) also shifted to lower values when sulphate was added to the solution. The fourth cathodic peak (C4) in the voltammogram of the 0 ppm sulphate artificial saline solution had a value of -0.438V/SCE. On the other hand, in the 200 ppm sulphate artificial saline solution, the potential value of the fourth cathodic peak was -0.774V/SCE. This new cathodic peak could be attributed to the reduction of CuS as shown by the following reaction:

ISSN 1466-8858 Volume 12, Preprint 42 submitted 30 June 2010

$$CuS \rightarrow Cu^{2+} + S^{2-} \quad (5)$$

Figure 6 shows the voltammogram of commercial alloy C70600 in artificial saline solutions with various amounts of sulphate (from 0 ppm and 2260 ppm sulphate) and in N.S. sea water. It can be observed that the same behaviour was observed when the concentration of sulphate in the solution was 800 ppm. The same peaks appeared in this range of sulphate and only a limited change in the position of the peaks was observed. The same behaviour was exhibited as with the 400 ppm sulphate artificial saline solution. Four anodic peaks (at +0.333 V/SCE, +0.488 V/SCE, +0.643 V/SCE, and +0.792 V/SCE potential values), and four cathodic peaks (at +0.07 V/SCE, -0.062 V/SCE, -0.444 V/SCE, and -0.499 V/SCE potential values) were observed. Peak A1 shifted to more positive values when adding 400 ppm or more sulphate to the solution. On the other hand, the second peak (A2) fluctuated in its value depending on the amount of sulphate in the solution.

Cathodic peak C1 was observed to shift to a lower potential value when the sulphate was 400 ppm in the artificial saline solution, and then it started to increase again at higher values of sulphate in the solution. At higher concentrations of sulphate, new peaks appeared as in the 800 ppm sulphate artificial saline solution for example, where there were three anodic peaks (with potential values of +0.366 V/SCE, +0.517 V/SCE, and +0.806 V/SCE), and five cathodic peaks (at +0.116 V/SCE, -0.082 V/SCE, -0.45 V/SCE, -0.79 V/SCE, -1.047 V/SCE, and -1.264 V/SCE potential values). Also, there was overlapping between the anodic and the cathodic paths when 800 ppm sulphate

ISSN 1466-8858 Volume 12, Preprint 42 submitted 30 June 2010

artificial saline solution used. This overlapping continued up to the addition of 2260 ppm sulphate to the artificial saline solution and was also observed in the N.S. sea water.

For 2260 ppm sulphate in the artificial saline solution, the peaks became more complicated and distorted, which made it difficult to separate the peaks from one another. The behaviour of the commercial alloy in the N.S. sea water was similar to the behaviour of the alloy in the 2260 ppm sulphate artificial saline solution.

It can be noted that the current density values of the anodic peaks were approximately constant up to a 400 ppm sulphate artificial saline solution, then they started to increase when more sulphate was added, causing a distortion in the cyclic voltammogram. These increases in the current density values can be explained by increases in corrosion rates under these conditions. This was consistent with the results of the linear polarization technique.

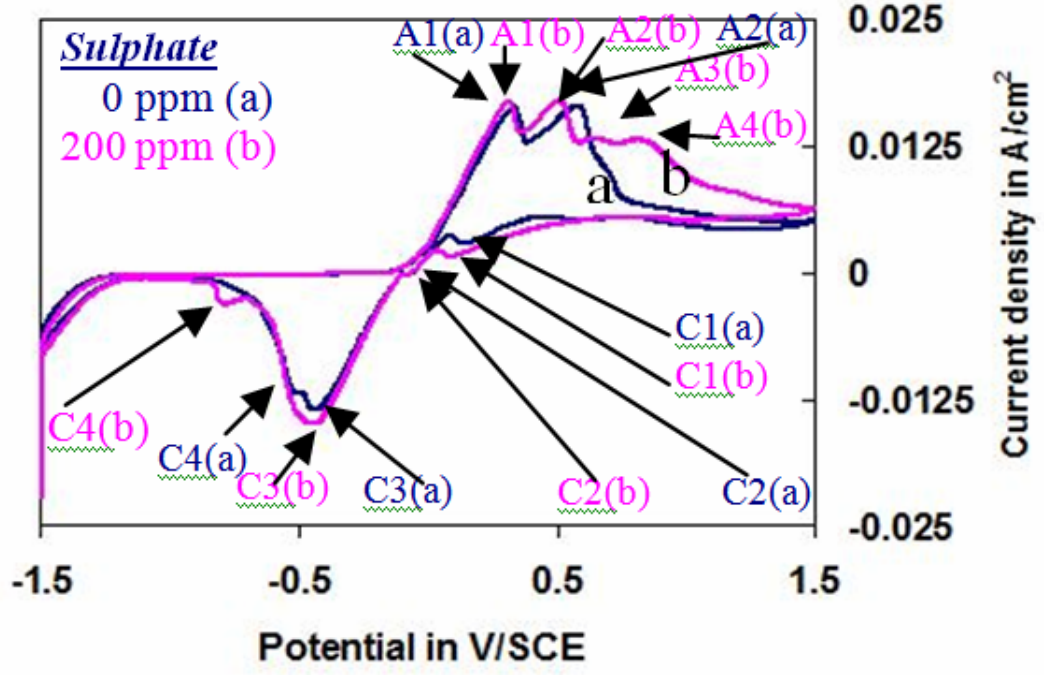

Figure 5. Cyclic voltammogram for the commercial alloy C70600 in 0 ppm and 200 ppm sulphate artificial saline solutions at a scan rate of 10 mV/s

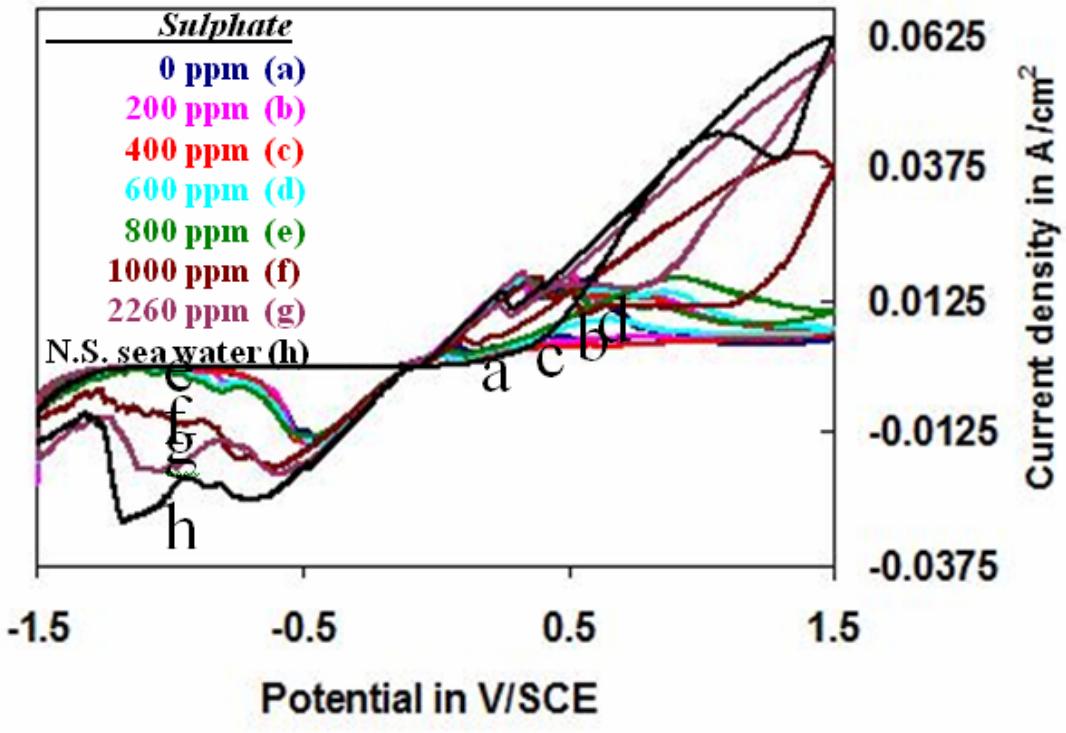

Figure 6. Cyclic voltammogram for commercial alloy C70600 in various artificial saline solutions and in N. S. sea water at scan rate of 10 mV/s

ISSN 1466-8858 Volume 12, Preprint 42 submitted 30 June 2010

An optical micrograph (Figure 7) shows clearly that the corrosion layer consists of two layers when a specimen of the commercial alloy was exposed to a 0 ppm sulphate artificial saline solution for twenty hours under open circuit potential: an outer layer of approximately 20 µm in thickness and an inner layer of approximately 80 µm in thickness were formed. A similar result was reported by previous studies [23, 24].

The outer layer is thin, cracked, has a weak adhesion to the inner layer, and has a dark blue colour. In contrast, the inner layer is thick, porous, shows better adhesion to the substrate surface, and has a golden brown colour. The outer layer colour converted to green colour if the specimen was exposed to air for a relatively long time. This colour also observed in a previous study [25].

Figure 8 shows the cracked outer layer when a 0 ppm sulphate saline solution was used. A similar microstructure was obtained in another investigation but with smaller structure [3]. EDS results show that this structure is richer in O, Cl, and Ni compared to the original base material. Based on the results of XRD and EDS, this layer consists mainly of mixed compounds which are CuCl, $Ni(ClO_4)_2.6H_2O$, and $Cu_2(OH)_3Cl$. Some NaCl precipitated from the solution on the outer layer as can be seen in the areas indicated by letter P in Figure 8.

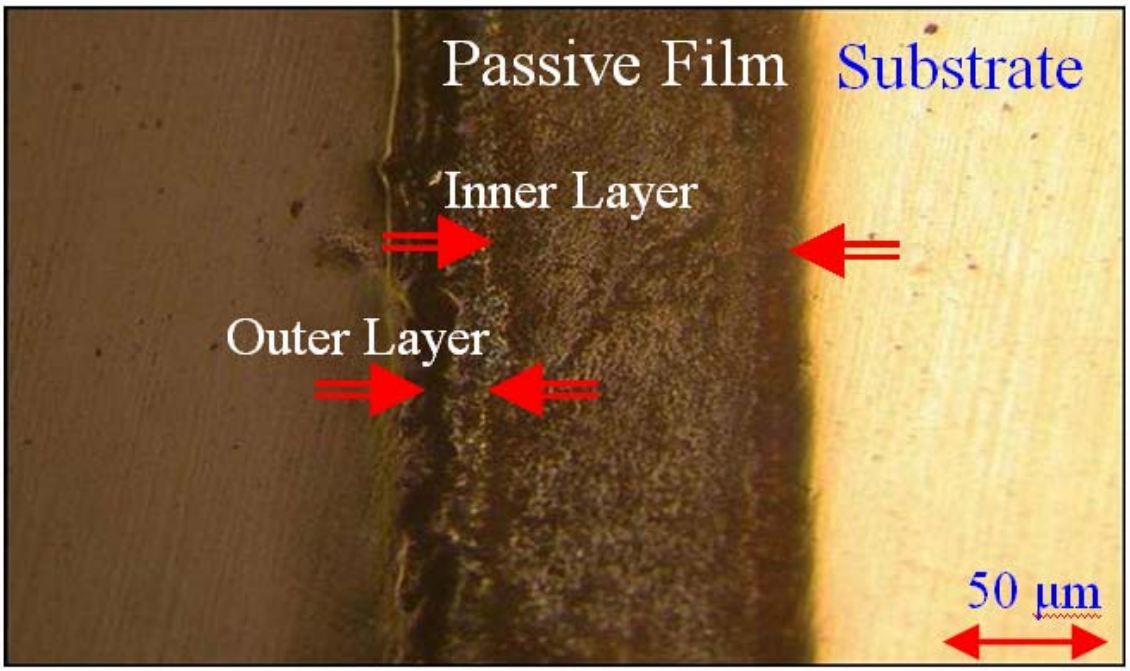

Figure7. An optical microscope image shows a cross section for passivated commercial alloy C70600 in a 0 ppm sulphate artificial saline solution.

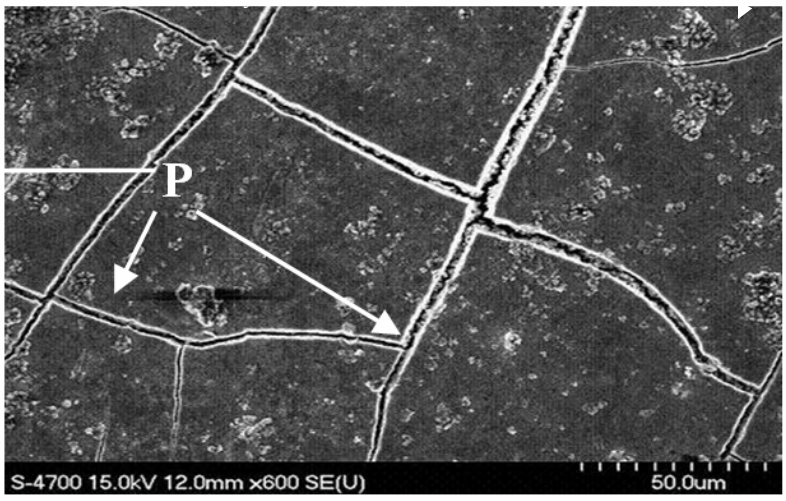

Figure 8. SEM micrograph of the outer layer of the corrosion product developed on a commercial alloy C70600 specimen exposed to a 0 ppm sulphate artificial saline solution where "P" represents NaCl precipitates

Figure 9 shows the inner porous layer of the corrosion product formed on commercial alloy C70600 when exposed for 20 hours to a 0 ppm sulphate artificial saline solution. The micrograph shows that the structure of this layer is porous and cracked.

ISSN 1466-8858 Volume 12, Preprint 42 submitted 30 June 2010

EDS results show that this structure is richer in Ni, O and Cl compared to the original base material. Based on the results of XRD and EDS, this layer consists mainly of $Ni(ClO_4)_2.6H_2O$.

The corrosion product film produced on the commercial alloy C70600 specimen that had been exposed to 2260 ppm sulphate artificial saline solution or N.S. sea water for twenty hours also consisted of two layers like the specimens exposed to a 0 ppm sulphate artificial saline solution. The outer layer of the corrosion product in the 2260 ppm sulphate artificial saline solution is shown in Figure 10. The EDS results show that the structure of this layer is richer in Ni, Fe, O, S, and Cl compared to the original base material. Also, based on the results of XRD and EDS, this layer consists mainly of mixed compounds which were observed on the commercial alloy exposed to a 0 ppm sulphate artificial saline solution, along with some new compounds which are FeOCl, FeS, CuS, and NiS. There was also a high amount of NaCl precipitate on the outer surface that was detected by EDS, and these precipitates are identified by the letter P.

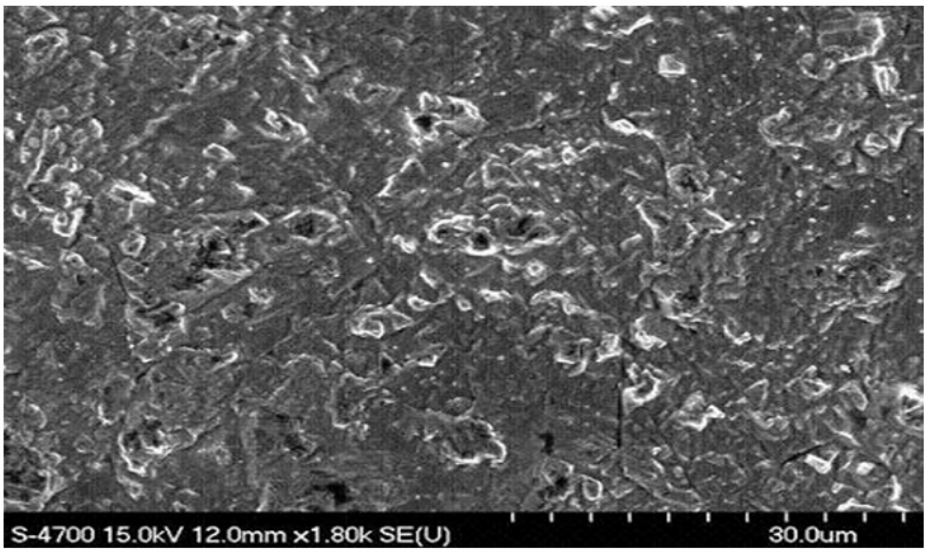

Figure 9. SEM micrograph of the inner layer of the corrosion product developed on commercial alloy C70600 in a 0 ppm sulphate artificial saline solution

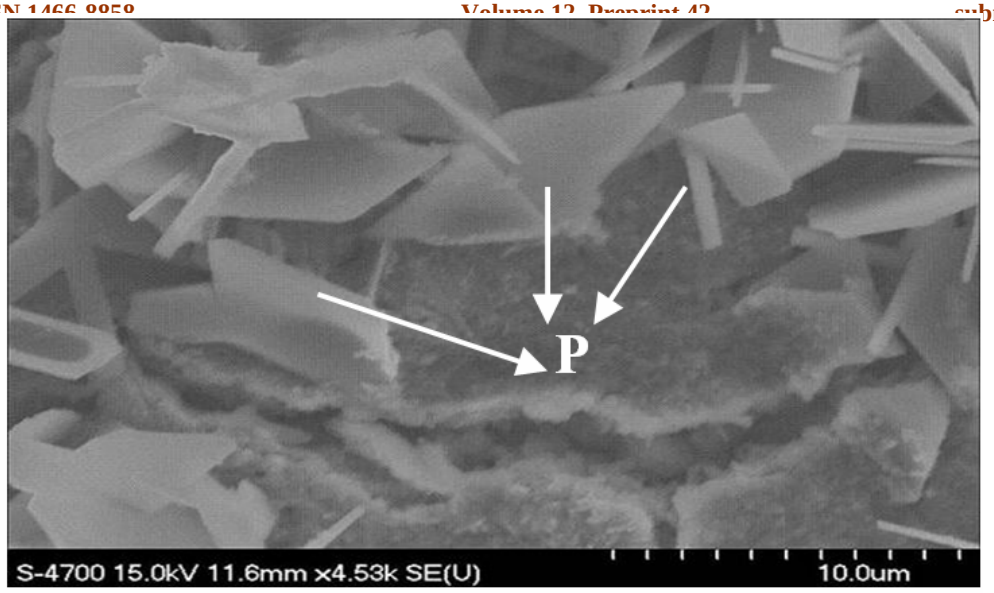

Figure 10. SEM micrograph of the outer layer of the corrosion product developed on commercial alloy C70600 in a 2260 ppm sulphate artificial saline solution, where "P" represents NaCl precipitates

The inner porous layer of the corrosion product formed on the commercial alloy exposed to a 2260 ppm sulphate artificial saline solution was richer in Ni, Fe, Cl, O, and S compared to the original base material. Based on the results of XRD and EDS, this layer consists mainly of mixed compounds, which are $Ni(ClO_4)_2.6H_2O$, $Cu_2(OH)_3Cl$, CuO, FeOCl, CuS, FeS, and NiS.

When using N.S. sea water, the structure of the outer layer was very similar to that shown in the case of the commercial alloy in an artificial saline solution consisting of 2260 ppm of sulphate. The EDS results show that the chemical composition of this layer was the same as that obtained by using 2260 ppm sulphate artificial saline solution. EDS results show that the structure of the inner layer of the passive film by using N.S. sea water is richer in Ni, Fe, Cl, O, and S compared to the original base material. Based on the results of XRD and EDS, this layer consists mainly of mixed compounds which are $Ni(ClO_4)_2.6H_2O$, $Cu_2(OH)_3Cl$, CuO, FeOCl, CuS, FeS, and NiS.

JCSE The Journal of Corrosion Science and Engineering
ISSN 1466-8858 Volume 12, Preprint 42 submitted 30 June 2010

EPMA equipped with EDS and WDS was used to investigate the nature of the corrosion film formed on the different samples. EDS was used for quick elemental scans to find out the elements available in the corrosion product (qualitative analysis). WDS is a complementary technique to the EDS where more accurate results can be obtained about the chemical composition of corrosion product (quantitative analysis).

Figures 11 and 12 are EPMA images of the cracked outer layers of the corrosion product formed on the commercial alloy exposed to a 2260 ppm sulphate artificial saline solution and the N.S. sea water, respectively. Crack surfaces appeared and the quantitative results for the corrosion product obtained from the WDS confirm the qualitative results obtained from the EDS which attached to the SEM, especially for those small unique precipitates spots which were confirmed to be NaCl crystals.

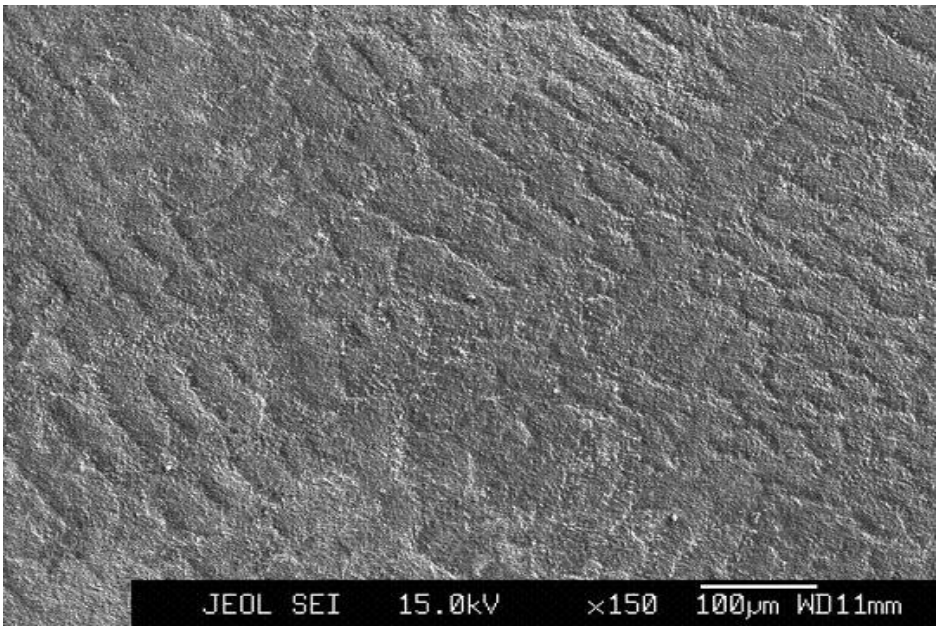

Figure 11. EPMA micrograph of the outer layer of the corrosion product developed on commercial alloy C70600 in N.S. sea water.

JCSE The Journal of Corrosion Science and Engineering
ISSN 1466-8858 Volume 12, Preprint 42 submitted 30 June 2010

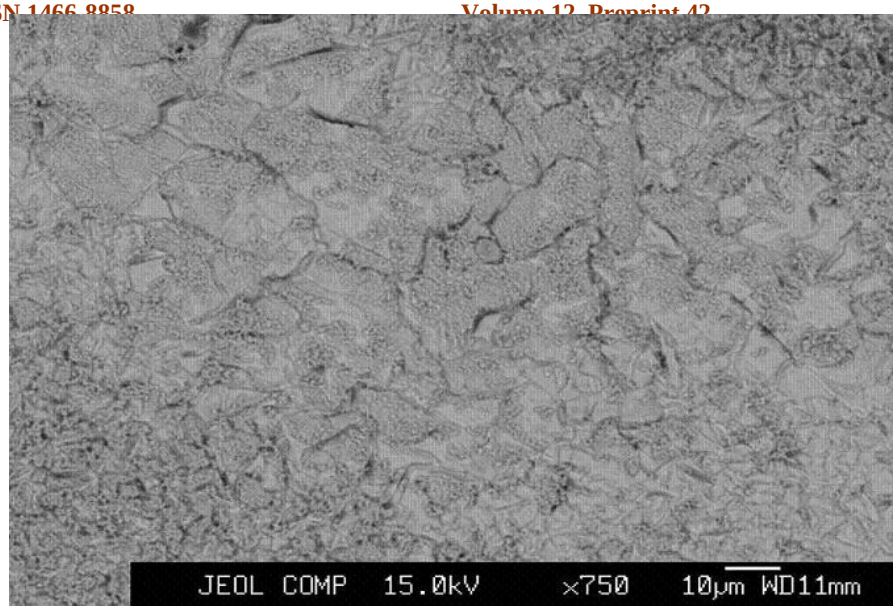

Figure 12. EPMA micrograph of the outer layer of the corrosion product developed on commercial alloy C70600 in a 2260 ppm sulphate artificial solution.

Conclusions

The electrochemical behaviour of the commercial alloy C70600 depends on the amount of sulphate in the saline solution. As the amount of sulphate in the artificial saline electrolyte increases above 400 ppm the ability of the passive film to protect the alloy is limited. Above the amount of 400 ppm sulphate, both the passivation current density and the passivation potential range decreased because of pitting corrosion tendency for the alloy.

The behaviour of the commercial alloy in sea water was similar to that in a 2260 ppm sulphate artificial saline solution. Small deviations were attributed to the fact that the N.S. sea water contains small amounts of substances in addition to sodium chloride and sodium sulphate that make up the artificial saline solutions.

The passive film formed on the commercial alloy C70600 was uniform in thickness and consisted of more than one layer. In solutions that contained no sulphate, the film

consists mainly of chlorides. In the presence of sulphate in the saline solutions the passive layer contains mainly chlorides and sulphides (FeS, NiS, and CuS).

Acknowledgments

The authors wish to acknowledge the Atlantic Innovation Found (AIF) and the Natural Science and Engineering Research Council (NSERC) for financial support. One of the authors (A.T.) would also like to acknowledge the financial support of the Libyan Education Ministry (LEM). The contribution of the Minerals Engineering Centre (MEC) in the chemical analyses is also acknowledged.

References

1. V. Callcut, "Copper Applications in Metallurgy of Copper and Copper Alloys", Innovation (online magazine), June 2000, http://www.copper.org/innovations/2000/06/cuni-marine-supreme.

2. C. Powell, "Copper-Nickel Alloys in Marine Environments", Corrosion and Prevention, 59, 2000, pp.1-8.

3. B. Syrett, "The Mechanism of Accelerated Corrosion of Copper-Nickel Alloys in Sulphide- Polluted Seawater", Corrosion Science, 21(3), 1981, pp. 187-209.

4. K. Efird, "Potential- pH Diagrams for 90-10 and 70-30 Cu-Ni in Sea Water", Corrosion, 31 (77), 1975, pp. 77-83.

5. P. Druska, H. Strehblow and S. Golledge, "A Surface Analytical Examination of Passive Layers on Cu/Ni Alloys: Part I. Alkaline Solution", Corrosion Science, 38(6),
1996, pp. 835-851.

6. S. Sayed, E. Ashour and G. Youssef, "Effect of Sulfide Ions on the Corrosion Behaviour of Al-Brass and Cu10Ni Alloys in Salt Water", Materials Chemistry and Physics, 78, 2003, 825-834.

7. M. Gavgali, I. Kaymaz, Y. Totik and R. Sadeler, "Corrosion Behavior of 90% Cu-

10% Ni Alloy at Different Rotation Speeds", Corrosion Reviews, 20(4-5), 2002, pp. 403-414.

8. J. Al- Hajji and M. Reda, "Corrosion of Cu-Ni Alloys in Sulfide- Polluted Seawater", Corrosion, 49 (10), 1993, pp. 809- 820.

9. H. Uhlig, "Corrosion Handbook", John Wiley & Sons, Inc., New York, 1948, pp. 3, 950-988.

10. D. Peters, "Review of Copper-Nickel Alloy Sheathing of Ship Hulls and Offshore Structure", Copper Development Association (Copper.Org.), http://www.copperinyourhome.org/applications/cuni/txt_asheating.

11. H. Dhar, R. White, G. Burnell, L.Cornwell, R. Griffin and R. Darby, "Corrosion of Cu and Cu-Ni Alloys in 0.5M NaCl and in Synthetic Seawater", Corrosion, 41(317), 1985, pp. 317-323.

12. K. Ismail, A. Fathi, and W. Badawy, "The Influence of Ni Content on the Stability of Copper-Nickel Alloys in Alkaline Sulphate Solutions", Journal of Applied Electrochemistry, 34, 2004, pp. 823-831.

13. A. El-Domiaty and J. Al Hajji, "The Susceptibility of 90 Cu-10 Ni Alloy to Stress Corrosion Cracking in Seawater Polluted by Sulfide Ions", Journal of Materials Engineering and Performance, 6(4), 1997, pp. 534-544.

14. K. Ismail, A. Fathi and W. Badawy, "Effect of Nickel Content on Corrosion and Passivation of Copper- Nickel Alloys in Sodium Sulfate Solutions", Corrosion, 60(9), 2004, pp. 795-803.

15. D. Vreeland and W. David, "Review of Corrosion Experience with Copper-Nickel Alloys in Sea Water Piping Systems", Materials Performance, (10), 1976, pp. 38-41.

16. C. Manfredi, S. Simson and S. de Sanchez, "Selection of Copper Base Alloys for Use in Polluted Seawater", Corrosion, 43 (8), 1987, pp. 458- 464.

17. J. Gudas and H. Hack, "Parametric Evaluation of Susceptibility of Cu-Ni Alloys to Sulfide Induced Corrosion in Sea Water", Corrosion, 35(2), 1979, pp. 259-264.

18. J. Gudas and H. Hack, "Sulfide Induced Corrosion of Copper Nickel Alloys", Corrosion, 35(2), 1979, pp. 67-73.

19. G. Kear, B. Barker, K. Stokes and F. Walsh, "Electrochemical Corrosion Behaviour of 90-10 Cu-Ni Alloy in Chloride-Based Electrolytes", J. of Applied Electrochemistry, 34, 2004, pp.659-669.

ISSN 1466-8858 Volume 12, Preprint 42 submitted 30 June 2010

20. R. North and M. Pryor, "The Influence of Corrosion Product Structure on the Corrosion Rate of Cu-Ni Alloys", Corrosion Science, 10, 1970, pp. 297-311.

21. B. Syrett and S. Wing, "Effect of Flow on Corrosion of Copper-Nickel Alloys in Aerated Sea Water and in Sulfide- Polluted Sea Water", Corrosion, 36 (2), 1980, pp. 73-84.

22. J. Mathiyarasu, N. Palaniswamy and V. Muralidharan, "An Insight Into the Passivation of Cupronickel Alloys in Chloride Environment", Indian Acad. Sci. (Chem. Sci), 113(1), 2001, pp. 63- 76.

23. H. Hack and H. Pickering, "The Influence of Corrosion Product Film Formation on the Corrosion of Copper-Nickel Alloys in Aqueous NaCl", Electrochemical Impedance: Analysis and Interpretation, ASTM STP 1188, J. Scully, D. Silverman, and M. Kendig, Eds., American Society for Testing and Materials, Philadelphia, 1993, pp. 220- 236.

24. M. Islam and S. Abo-Namous, "Electron Microprobe Analysis of Metal/ Film Interface and Surface Film Formed on 90/10 Cu-Ni Alloy During SCC Tests in 1 M Sulfide Solution", Corrosion, 47 (9), 1991, pp. 654-658.

25. J. Al Hajji and M. Reda," On the Effect of Common Pollutants on the Corrosion of Copper- Nickel Alloys in Sulfide Polluted Seawater", J. Electrochem. Soc., 142(9), 1995, pp. 2944-2953.